Jets and loops from the nucleus of NGC 2655

Keel, W.C.; Hummel, E.

Astron. Astrophys. 194, 90–98 (1988)

ASTRONOMY AND ASTROPHYSICS

Jets and loops from the nucleus of NGC 2655

W. C. Keel [1,2,*] **and E. Hummel** [3,4]

[1] Kitt Peak National Observatory, National Optical Astronomy Observatories**
[2] Sterrewacht Leiden, Postbus 9513, 2300 RA Leiden, The Netherlands
[3] Max-Planck-Institut für Radioastronomie, Auf dem Hügel 69, D-5300 Bonn 1, Federal Republic of Germany
[4] Nuffield Radio Astronomy Laboratories, Jodrell Bank, Macclesfield, Cheshire, Sk 11 9DL, UK

Received August 20, accepted October 22, 1987

Summary. We present narrow-band optical images, long-slit spectra, and radio maps of the peculiar early-type galaxy NGC 2655. A large (6 kpc) and complex emission-line region is present, showing loops, filaments, and a strong off-nuclear knot. Emission-line ratios indicate that all of this gas is excited by processes other than photoionization by hot stars. Its kinematics cannot be fully specified from our data; local motions of several hundred km s^{-1} exist. The radio structure includes small-scale jets from the nucleus, and an extended counterpart to the strongest off-nuclear optical emission region. In this emission region, the thermal and radio-emitting plasmas are in rough pressure balance. We suggest that the optical emission is powered by the radio plasma, either via shocks or by a local ionizing continuum. This system would then be a low-luminosity version of some powerful radio galaxies with discrete high-ionization emission regions found well away from their nuclei.

Key words: galaxies: NGC 2655 – jets of galaxies – radio galaxies – nuclei of galaxies – evolution of galaxies

1. Introduction

The role of radiative energy transport in active galactic nuclei has long been recognized, but there are recent indications that energy is also transported mechanically, via shocks or particle flows, in at least some objects. For example, the structure and kinematics of ionized gas in the central region of M 51 seem to require that most of the energy output from the nucleus is converted into bulk motion of the gas (Ford et al., 1985; Goad and Gallagher, 1985). Evidence for collisional energy input to emission regions in 3C 293 has been presented by van Breugel et al. (1984). Most recently, twin emission-line regions in the type 2 Seyfert galaxy NGC 5929 have been used as evidence for a twin-beam source in this nucleus (Keel, 1985a). We report here observations of an additional nearby galaxy in which the nucleus powers a complex, extended region of plasma, and in which nonradiative processes seem important.

Send offprint requests to: E. Hummel

* Now at the Dept. of Physics and Astronomy, University of Alabama, P.O. Box 1921, Tuscaloosa, AL 35486, USA
** Operated by AURA, Inc., under contract with the National Science Foundation

NGC 2655 is a bright galaxy with peculiar morphology. The central region is amorphous, with a strong condensation. Deep images show faint arms or ripples on the envelope. A number of dust patches are present, mostly along the projected minor axis. Published classifications include Sa pec (Sandage and Tammann, 1981) and S0/a (de Vaucouleurs et al., 1976). The nuclear radio emission is unusually strong and compact for a spiral galaxy (van der Hulst et al., 1981; Crane, 1977; Hummel et al., 1984). This fact prompted optical work showing the peculiar Hα structures described below, and led to the imaging, spectroscopy, and radio mapping reported here. An independent detection of the extended Hα structure has been reported by Dahari et al. (1986).

We discuss in turn our observations and their direct implications, the nature of the extended emission-line region and a prominent emission-line and radio knot, and comparison with phenomena found in more luminous active systems.

2. Observations

2.1. Optical images

Early images with the Kitt Peak National Observatory (KPNO) Video Camera system showed a loop and filaments in Hα. To study this structure in more detail, a TI 800 × 800 CCD was used with the KPNO 2.1-m telescope. Exposures were obtained through an interference filter with peak transmission at 6606 Å, FWHM 76 Å (15^m) and broad-band R and B filters (5^m each). From these, a difference image reflecting only Hα + [N II] emission was generated (Fig. 1). A wealth of detail is visible, covering a region nearly 30″ across. Most prominent is a loop structure north of the nucleus, which may continue to the south and form a complete (projected) ellipse. This loop is not centered on the nucleus; in fact, the nucleus is projected onto it. The nuclear emission is extended (with embedded knots) to the west. A detached, resolved emission region appears to the ESE, at 14″.5 from the nucleus in position angle 114°.

Comparison with the broad-band appearance of NGC 2655 shows that the spectacular appearance in Hα is not dominated by effects due to dust lanes.

2.2. Optical spectroscopy

Slit spectra have been obtained covering the nucleus, loop, and ESE knot of NGC 2655. The Cryogenic Camera was used at the 4-m Mayall telescope, with a grism having 600 lines mm^{-1}. This

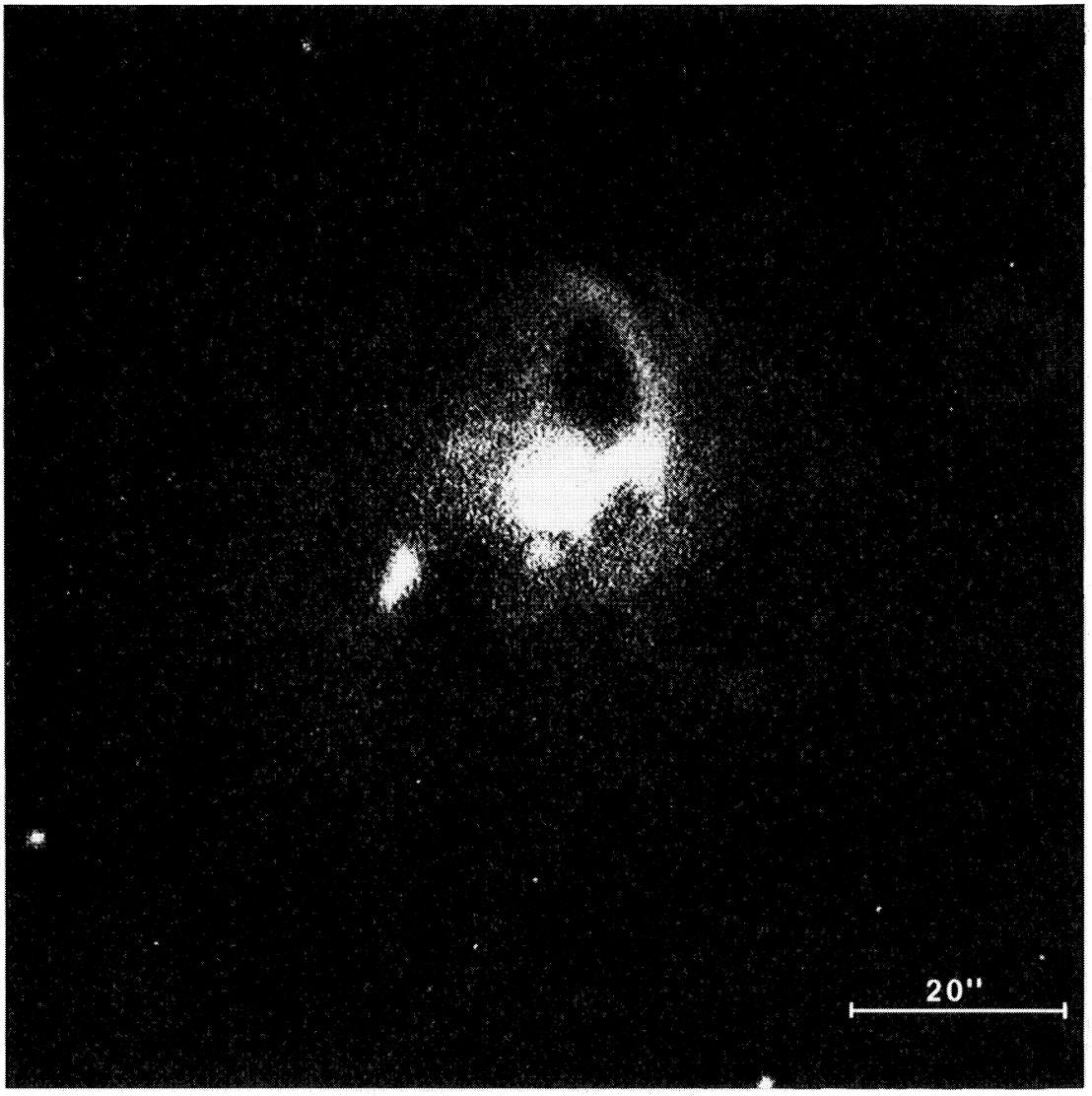

Fig. 1. Hα + [N II] image of NGC 2655, after subtracting a continuum image. Intricate extranuclear structure is present, including a strong knot 14.″5 to the ESE of the nucleus, and a loop or ring to the north (top). The image is 104″ square, corresponding to 8 kpc for a distance of 16 Mpc

gave a spectral coverage of 4600–7900 Å, at a resolution ~15 Å. Observation of arc lamps immediately before and after the galaxy spectra gave an absolute wavelength scale good to ~30 km s^{-1} in velocity. Position angles 0° and 114° were observed for 10^{m} each, with a slit width of 2.″5. The instrumental response was measured and removed through observations of the standard star HZ 2. Reduction to arrays of flux (F_λ) versus position along the slit was done using the mapping and distortion-removal routines in the RV package of the IPPS system.

From these spectra, it is clear that *all* the emission-line structures seen in Fig. 1 are low-ionization features not produced by star-forming regions (in fact, it is not clear that any normal H II regions have been detected in NGC 2655, consistent with the relatively weak far-IR emission found by IRAS; Joint IRAS Science Working Group 1985). As seen in Fig. 2a the nuclear spectrum is that of a LINER, as defined by Heckman (1980); [O I] λ6300 is strong, while [O III] λ 5007 is weak; this was implicit in the line strengths reported by Andrillat et al. (1972). The most striking feature of the extended nebulosity is its spectral similarity to that at the nucleus (Fig. 2b and c). The knot ESE shows some differences, with narrow lines and slightly higher ionization (Fig. 2c). This object resembles a LINER in its own right, except that we find no continuum counterpart; there is no detectable concentration of stars here, so that this is not the nucleus of a merging galaxy. Line ratios at various of these positions are given in Table 1.

Velocities have been measured from the spectra. We used the lines [N II] λ6584 and [O III] λ5007 for gas kinematics and NaD $\lambda\lambda$5890, 5896 as indicators of the stellar kinematics. Even at the relatively coarse scale of 3.5 Å/pixel used here, velocity centroids are accurate to $\leqq$0.3 Å = 50 km s^{-1}, but spurious results may be obtained when unresolved velocity systems overlap. The derived velocity distributions (Fig. 3) are quite complex, and show little coupling between stars and gas. Velocity gradients in the gas are seen in the immediate vicinity of the nucleus. A jump in radial velocity is present at the *W* edge of the loop. Most interesting is a gradient along the ESE knot, indicating rotation or ordered shear within the knot.

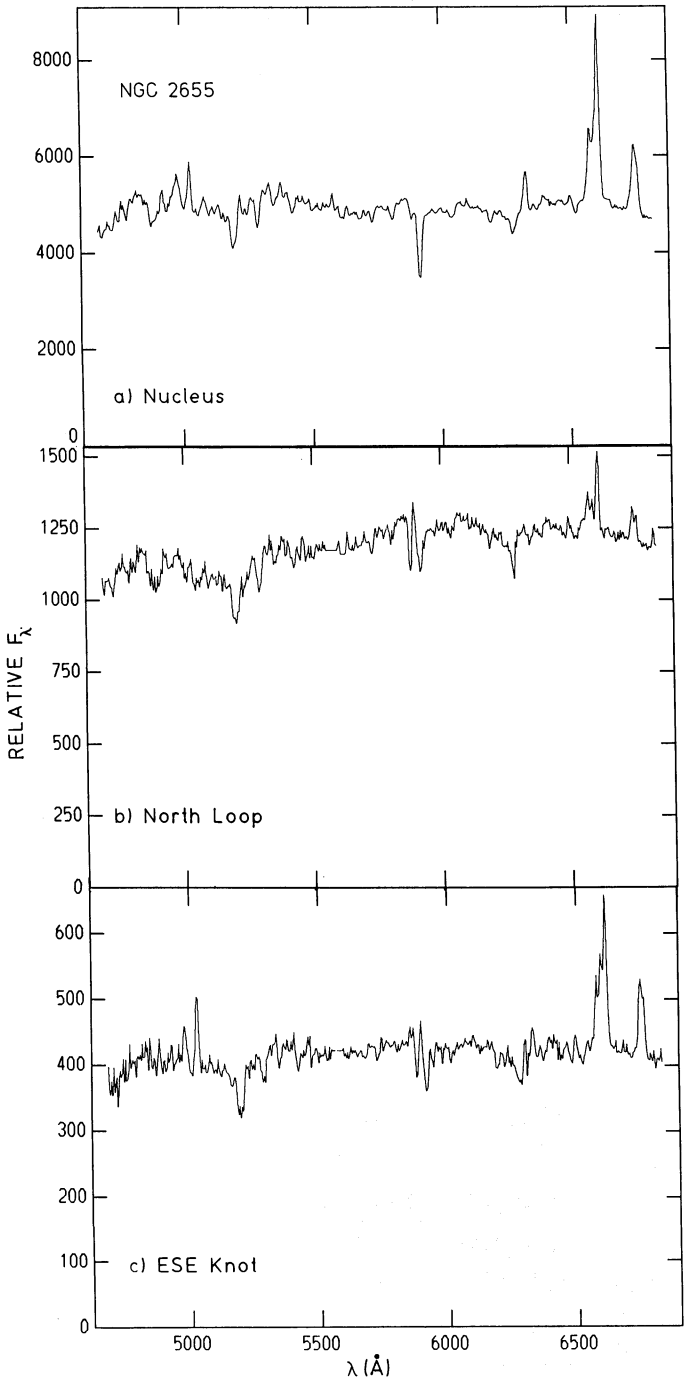

Fig. 2. (a) Optical spectrum of the NGC 2655 nucleus. Low-ionization emission lines are prominent, superimposed on an old stellar population. (b) Spectrum of a region 9–18″ *N* of the nucleus, with similar emission-line properties. (c) Spectrum of the ESE emission knot, showing emission lines of slightly higher ionization and smaller velocity width than the nucleus

The stellar velocity structure is broadly consistent with a rotating disk whose axis lies close to the line of sight ($\Delta V \sim 120$ km s^{-1} near the major axis). The curves are not, however, symmetric about the nucleus, suggesting that some kind of dynamical disturbance has taken place. The optical morphology at faint levels may also indicate a recent disturbance (merger?), and HI maps also show a disordered velocity field in the outer regions (2′ from the nucleus; Shane and Krumm, 1983; Shane, in preparation).

Table 1. Emission-line ratios in NGC 2655

	Nucleus	N. Loop	ESE Knot
[N II] λ6593/Hα	2.20	1.16	1.26
[O I] λ6300/Hα	0.40	<0.4	0.20
[S II] λ6717, 6731/Hα	1.37	0.71	1.08
[S II] λ6717/λ6731	1.04	1.3:	1.35
[O III] λ5007/Hα	0.8	<0.5	0.64

The long-slit data have been be supplemented with aperture spectrophotometry of the nucleus, useful in checking the absolute flux scale of our other data and in extending wavelength coverage of the nucleus. NGC 2655 was observed with the Lick 3-m telescope and IDS system (courtesy of J.S. Miller), using 3″.7 circular apertures. The data were also analyzed with a spectrum-synthesis code to determine line ratios free of contamination by stellar absorption features (Keel, 1983), with results included in Table 1. Larger aperture measures used the Intensified Reticon Scanner (IRS) at the KPNO #1 0.9-m telescope and 7″ apertures; the total Hα flux in this region is 1.33 10^{-13} erg cm^{-2} s^{-1}.

2.3. *Radio mapping*

NGC 2655 was observed with the Very Large Array (VLA) of the National Radio Astronomy Observatory (NRAO)[1]. A description of the VLA is given by Thompson et al. (1980) and Napier et al. (1983). A summary of the observations is given in Table 2. As phase calibration we used at both dates the source 0836+710 whose position is known with an accuracy of better than 0″.1. On January 6 1984 we obtained, using 3C 286 as the flux density calibrator, a flux density for 0836+710 at 4.86 GHz of 2.49 Jy, in close agreement with the flux density we used on April 13.

The edited visibility data were Fourier-transformed and the resulting maps were "cleaned" (Clark, 1980) in order to remove the sidelobes of the synthesized beam. The full resolution maps at 1.46 GHz and 4.86 GHz of January 6 so obtained have half power beam widths (HPBW) of 4″ and 1″.2 respectively and rms noises of 0.15 mJy/beam and 0.06 mJy/beam respectively. The 4.86 GHz map obtained on April 13 has an HPBW = 4″ and rms noise of 0.1 mJy/beam. To improve sensitivity for more extended structure we applied a weighting function to the 1.46 GHz January 6 observation and the 4.86 GHz April 13 observation so that the resulting HPBW = 8″ and the rms noises are 0.3 mJy/beam and 0.1 mJy/beam respectively.

In Fig. 4 we show the 1″.2 resolution map at 4.86 GHz. Also shown is the 0″.5 resolution map obtained by Hummel et al. (1984). The latter shows an *S*-shaped component and a rather compact nuclear source (half power size = 0″.4 × 0″.2 at p.a. = 42°). The 1″.2 resolution map shows in addition to the nuclear source a second component at 14″ ± 1″ from the nucleus at p.a. = 117° ± 4°. The relevant parameters of the two radio components are given in Table 3. Figure 5 shows the 4″ and 8″ resolution 4.86 GHz maps. They show the secondary component more clearly. In addition they show two extensions from the main component, one at p.a. = 282° which curves to the north and one at p.a. = 2°, and

[1] The VLA is a facility at NRAO, which is operated by Associated Universities, Inc. under contract with the National Science Foundation.

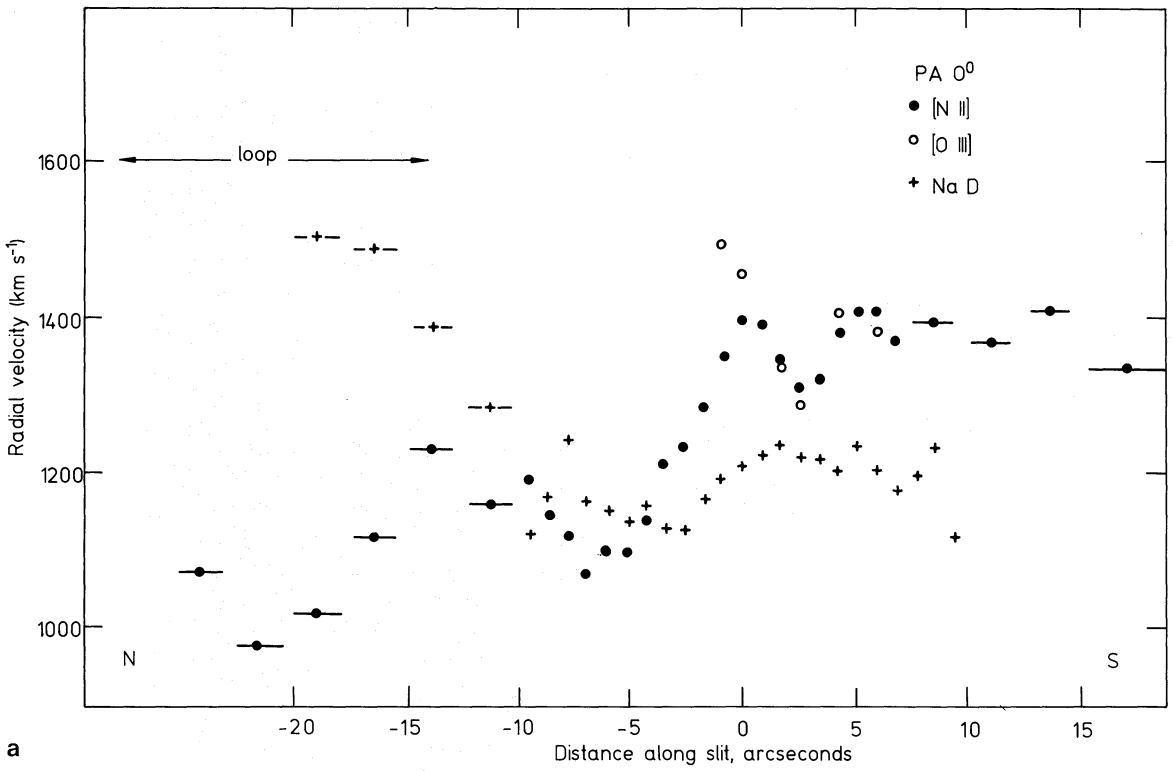

a

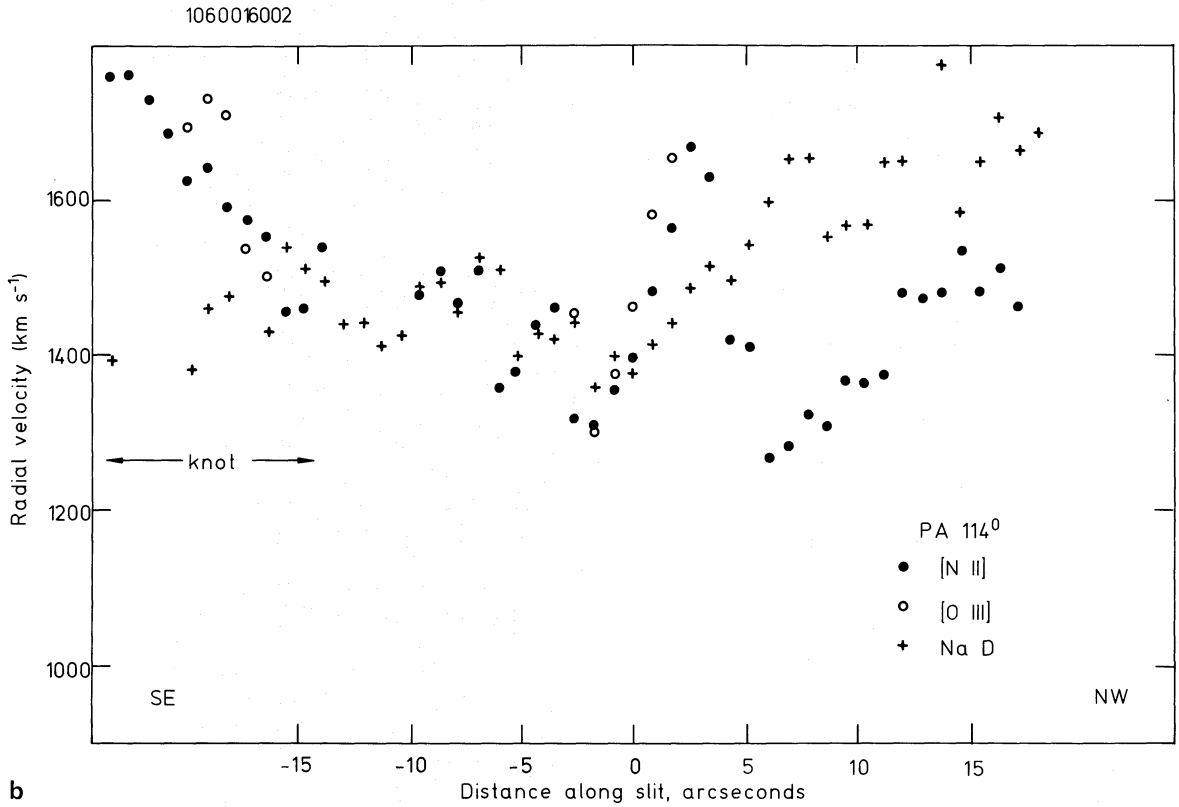

b

Fig. 3a and b. Velocity distribution along our spectroscopic slit position for starlight (+), [N II] emission (·), and [O III] emission (○). Positions of features from Fig. 1 are marked. **a** Position angle 0°, passing through the loop. **b** P.A. 114°, passing through the ESE knot

Table 2. Radio observations of NGC 2655

Date of observation	1984 Jan. 6	1984 Jan. 6	1984 Apr. 13
Frequency (GHz)	1.49	4.86	4.86
Bandwidth (MHz)	100	100	100
Observing time (min)	40	40	40
Shortest spacing (m)	210	210	63
Longest spacing (km)	11.4	11.4	3.4
Flux density calibrator	3C 286	3C 286	0936+710
Flux density of calibrator (Jy)	13.7	7.3	2.4[a]

[a] Obtained from flux density monitoring at VLA

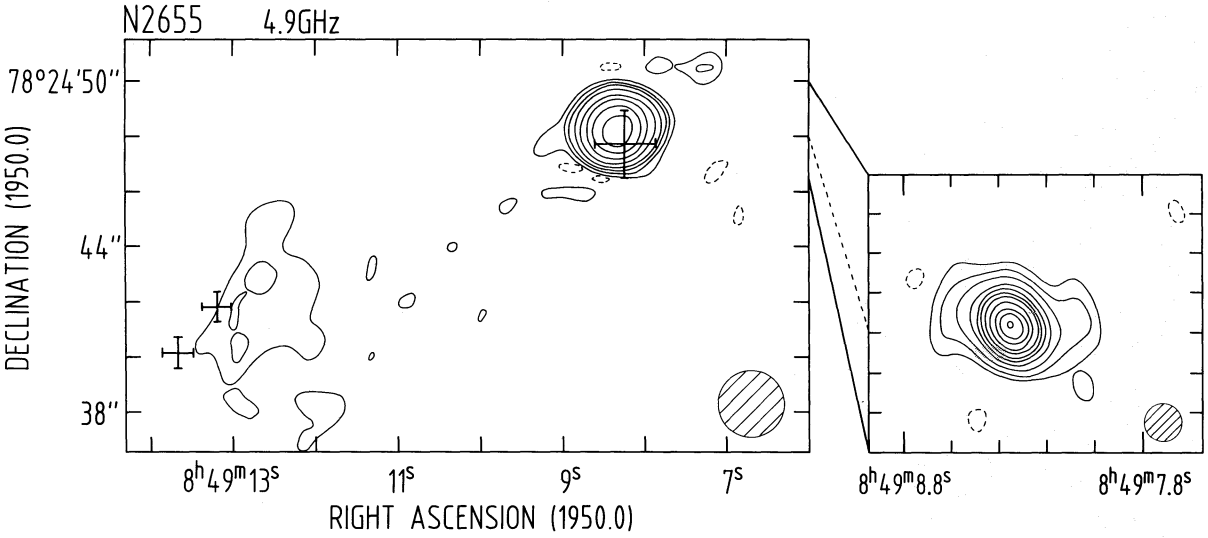

Fig. 4. Maps of NGC 2655 at 6 cm, with 1".2 resolution (left) and at 0".5 resolution (right, from Hummel et al., 1984). Extensions to the nuclear emission, and a feature roughly coincident with the ESE emission knot, are apparent. The optical positions of the nucleus and of the two components of the ESE knot are indicated. Contour levels are (left) −0.15, 0.15, 0.3, 0.6, 1.2, 2.5, 5, 10, and 20 mJy/beam, and (right) −0.25, 0.5, 1, 2, 4, 6, 8, 10, 14, 18, 22, and 26 mJy/beam

Table 3. Radio results for NGC 2655

	Main component	Secondary component
Right ascension (1950.0)	$08^h49^m08^s.34$	$08^h49^m12^s.66$
Declination (1950.0)	78°24'48".5	78°24'43".0
Flux density at 1.46 GHz (mJy)	94 ±2	13.0±0.5
Flux density at 4.86 GHz (mJy)	43 ±1[a]	5.5±0.2
Deconvolved half power size (arcsec)	0.7±0.1[b] (±0.5)	6.2×4.5 (p.a.=0°)
Spectral index: Total	−0.66±0.04	−0.73±0.06
Peak[c]	−0.67±0.01	−0.55±0.06

[a] 36±1 mJy is in nuclear component of size 0".4×0".2 (42°), Hummel et al. (1984)
[b] From 1".2 resolution 4.86 GHz observation, includes S-shaped component
[c] From 4" resolution 4.86 GHz and 1.46 GHz maps

there seems to be a bridge of emission between the main and secondary components.

Since the 1.46 GHz January 6 observation and the 4.86 GHz April 13 observations were made, in terms of wavelengths, with almost identical array configurations, these observations can be used to determine reliable spectral indices. The main component has a spectral index[2] of $\alpha = -0.66 \pm 0.04$ and there is no indication of spectral index variations. This is *not* the case for the secondary component. There the spectrum for the total emission ($\alpha = -0.73 \pm 0.06$) is significantly steeper than the spectrum for the inner part ($\alpha = -0.55 \pm 0.06$). This suggests strongly that the radio spectrum steepens going outwards within the secondary component.

Alignment of optical and radio maps was facilitated by measurement of the precise position of the optical nucleus with respect to 8 nearby SAO stars, using a blue-sensitive plate taken with the 0.9-m Crossley reflector at Lick Observatory; only the inner few arcseconds were saturated on this plate, allowing an accurate determination of the center. The optical nucleus is at (1950) $8^h49^m8^s.26 \pm 0.34$, +78°24'47".7±1".2; this is coincident with the VLA core position to well within the errors (formal offsets $0^s.08$ in α, 0".8 in δ. We thus take these cores to be coincident.

[2] Spectral index α defined as $S \propto \nu^{\alpha}$

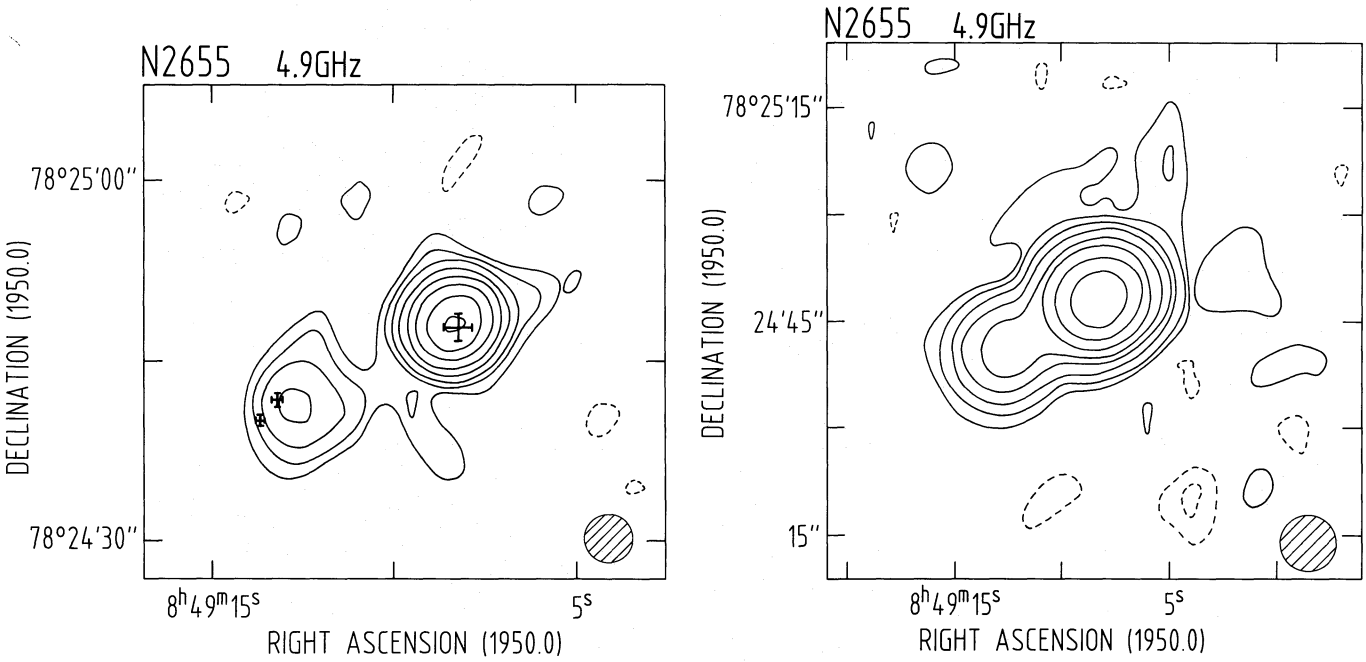

Fig. 5. 6-cm maps at resolution of 4″ and 8″, showing the secondary component associated with the ESE knot, and extensions of the nuclear source. The optical positions of the nucleus and of the two components of the ESE knot are indicated. Contour levels are (left) −0.25, 0.25, 0.25, 1, 2, 3, 4, 5, 6 mJy/beam and (right) −0.3, −0.15, 0.15, 0.3, 0.6, 1.2, 2.5, 5, 10, and 20 mJy/beam

3. Aspects of the nuclear region of NGC 2655

3.1. *The nucleus*

The nuclear spectrum is that of LINER (Heckman, 1980), with strong [O I], [S II], and [N II] lines but relatively weak [O III]. The emission lines are clearly resolved even in the 20 Å-resolution Cryogenic Camera spectra, implying a width of order 500 km s^{-1}. The Hα luminosity from the innermost 3″.7 (diameter), from an observed flux of 1.3 10^{-13} erg cm^{-2} s^{-1} and assuming a distance of 16 Mpc, is 5 10^{38} erg s^{-1}. The total luminosity in observed emission lines is about 10 times this, due to the prominence of forbidden-line emission. No broad component of Hα, such as would directly imply the presence of a weak Seyfert 1 nucleus, was detected to a level of ~10% of the observed Hα flux over a 100-Å (4500 km s^{-1}) range, below the levels seen in the "dwarf Seyfert" nuclei discussed by Filippenko and Sargent (1985). The strong forbidden lines and low overall ionization state suggest a role for photoionization by a weak flat-spectrum source in the nuclear gas (e.g., Keel, 1983), but similar properties may be produced by shocks (see Keel, 1985 and references therein). Note that we would not expect to see a flat-spectrum ($\alpha \approx -1$), isotropic continuum source of sufficient UV luminosity to power the nuclear emission lines, as it would be very weak compared to the bulge starlight even in a small aperture about the nucleus.

3.2. *Velocity structure in the extended emission-line regions*

The velocity information, together with the Hα image, may be used to identify various emission regions in velocity and position. Either a jump in emission-line velocity or departure from the local stellar velocity might be evidence of a change in the dominant emitting component. These are discussed starting near the nucleus and working outward.

The nuclear region ($r < 3''$) shows a strong velocity gradient both in stars and gas. The emission-line gradient is larger, with the difference across this region reaching 200 km s^{-1}. The emission-line gradient, like that in stellar velocities, extends further *W* than *E* of the continuum peak, approximately along the Hα extension from the nucleus. The gas motions here might reflect either directed radial flow or an inner disk, whose dynamics match the local stellar component; in this case, the lower stellar velocity gradient would be due to the different weighting along the line of sight. The emission region 6″ *S* of the nucleus shows a velocity similar to that at the nucleus, but intervening dips in velocity indicate that it is a separate structure from the nuclear emission, and that an emission-line component with velocity similar to that of the stars appears between them.

A region of matching stellar and gas radial velocities appears from 3″ to 10″ ESE of the nucleus (in the direction of the ESE emission knot). This corresponds to a smooth "halo" in the Hα image. The two parts of this emission evident in Fig. 4b might reflect inner spiral structure (if this is in fact a spiral galaxy) or the effect of an internal dust cloud.

The emission knot NW of the nucleus, along the Hα loop, is blueshifted with respect to the nucleus and its environs, and the local stellar velocities. A gradient is present, in the sense that the blueshift (300 km s^{-1}) is greatest on the inner side and the velocities approach at the outside; a range ~225 km s^{-1} is observed.

The emission loop, where it has been observed spectroscopically north of the nucleus, shows a blueshift of as much as 400 km s^{-1} with respect to the starlight, or 200 km s^{-1} with respect to the nucleus; the highest velocities are seen at larger projected distances. A continuity with the NW knot is plausible.

The strong emission knot ESE of the nucleus is seen to be composed of at least two main pieces in the Hα image. A continuously increasing redshift from NW to SE is present, with a

range of 250 km s^{-1} detected. The velocity structure is continuous, suggesting a large-scale shear or rotation of the whole structure (since it may be said to show a coherent "rotation curve") rather then different velocities for each part of the Hα structure.

As puzzling as the Hα structure is in itself, the velocity data make it even more difficult to interpret the gas motions here. The most conservative view would associate the emission in the nucleus and the quiescent background with a gaseous disk rotating in approximately the equatorial plane of the galaxy (though there does not seem to be enough of a thin disk to make this a very well-defined plane). However, the three off-nuclear emission blobs and the loop require a less usual explanation; their origin is probably linked to activity at the nucleus itself.

As the most coherent structure observed, the loop may be subjected to a crude kinematic analysis from these data. Assuming it to be circular and in regular motion (for neither of which conditions we have direct evidence) the space velocity of the ring may be decomposed into a rotational component V_t and an expansion or contraction velocity V_r. When viewed on the sky so that the ring makes an angle i with the line of sight, these result in a kinematic line of nodes shifted by an observed angle $\tan^{-1}(V_r/V_t)$ $\sin i$ with respect to the projected major axis of the ring. These sense of the shift relative to the direction of rotation indicates whether expansion or contraction is present, if the near and far sides of the ring are known (the usual ambiguity in studies of this type).

If the loop has no center-of-mass motion in the line of sight (another assumption), we may adopt the nuclear velocity as that of its center. Then, from the data of Fig. 4, a shift between the projected major axis and line of nodes of at least 45° must be present. In this simple model, the ring is expanding or contracting as fast as it is rotating. The difficulty of producing a coherent ring off the nucleus which will contract as a whole leads us to propose that the loop is an expanding ring (in which case the near side is to the west).

3.3. Ionization of the extended emission-line region

The ionization state of the circumnuclear gas suggests that it is intimately related to events in the nucleus. Such line ratios are not produced by OB stars as found in normal H II regions, but require a dilute power-law radiation field or shocks for their production. Photoionization is plausible in the inner few hundred parsecs for LINERS in general (Keel, 1983; Filippenko and Halpern, 1984). For very extensive emission regions such as the loop and outer knots in NGC 2655, however, a more local energy input such as that by shocks seems indicated, particularly since the [S II] ratio in the knots indicates an electron density of at least 100 cm^{-3}. Any ionizing continuum capable of sustaining the required ionization parameter U = ionizing photons/particle (in the range 10^{-3}–10^{-4}, from the emission-line ratios) would have to be very strongly beamed so as not to be detected optically at the nucleus. The same argument has been detailed for the emission-line filaments in M87 by Ford and Butcher (1979).

The means of ionization for the loop and knots might then be shocks or photoionization by a flat-spectrum UV continuum produced in situ (for the knots). There are no clear spectroscopic distinctions in spectra of this kind, so that for the present we must consider quite general pictures for this object. The very fact that gas in the knots is ionized is more important than which of these modes is dominant. From both images and spectra, we may set an upper limit of $2\ 10^{-16}$ erg cm^{-2} s^{-1} Å^{-1} for any featureless continuum associated with the SE knot. For a ν^{-1} spectrum typical of synchrotron features, this limit corresponds to $4\ 10^{40}$ erg/s from the Lyman limit to the near-IR. This limit is not low enough to rule out a continuum capable of producing the observed line emission through photoionization, so that we have no direct argument in support of either of these suggested energy-input mechanisms.

4. The ESE emission knot – The working surface of a jet?

The emission knot seen well away from the nucleus in Fig. 1 has no close analog among nearby, well-studied galaxies. Both in its optical properties (strong low-ionization emission, morphology, lack of a continuum counterpart) and in its coincidence with a relatively strong off-nuclear radio source, it is not described by simple models for emission from galactic nuclei. The level of activity observed in the nucleus of NGC 2655, especially in the radio, does suggest that the off-nuclear emission knot owes something to events at the nucleus.

Since the density in the knot is not securely measured (the [S II] line ratio is near the low-density limit), additional constraints on n_e and the ionization parameter due to radiation from the nucleus must be considered. First, the total amount of material in the knot must be sufficient to produce its observed emission-line luminosity at an appropriate temperature (0.7–1.4 10^4 K). For a Balmer line with emissivity $\varepsilon(T)$, this gives

$$L(\text{line}) = n_e^2\, f\, V\, \varepsilon(T)$$

for a cloud of volume V and filling factor f. The requirement $f \leqq 1$ gives $n_e \geqq 4$ for the knot. Second, the line luminosity of the knot and its covering factor as viewed from the nucleus ($\Omega/4\pi \simeq 5\ 10^{-3}$, again assuming a depth comparable to the observed dimensions) may be compared with the Lyman continuum luminosity inferred for producing the nuclear emission lines; if the knot emits more that $\Omega/4\pi$ of the nuclear UV continuum luminosity, in observed lines, an isotropically radiated continuum cannot be responsible. A stronger constraint would allow for unobserved emission lines in a model-dependent way; we retain the simpler, more conservative comparison here. The knot's line luminosity is observed to be $5\ 10^{38}$ erg/s, and the inferred nuclear continuum has a total Lyman continuum luminosity of order $2.4\ 10^{41}$ erg/s (evaluated for a ν^{-1} spectrum up to the He II Lyman edge, if all the nuclear line emission is due to photoionization). On energetic grounds alone, then, the observed line emission could (just) be powered by an isotropic ionizing source at the nucleus, if the density in the knot is high enough for it to absorb all the incident UV photons (i.e., the knot is optically thick in the Lyman continuum).

A third, approximate constraint considers ratios between the knot and emission-line material seen near the nucleus (at distances of about 2″ or 150 pc projected). For comparable ionization parameters (noting that this is observed to be slightly higher in the knot than the nuclear gas), the distances and densities of the nuclear (N) and knot (K) gas must satisfy

$$\frac{n_e(K)}{r_K^2} = \frac{n_e(K)}{r_N^2}$$

so that a particle density $1.8\ 10^{-2}$ or less of that in the nuclear gas (which is near 300 cm^{-3}, from the [S II] lines) is needed for this type of photoionization in the knot. This implies $n_e < 5.5$ cm^{-3}; the small overlap of this range with that allowed by the absolute lower limit of 4 cm^{-3} from volume emissivity (above) is a strong suggestion that photoionization, if a dominant energy source in

the knot, is due to an in situ source, or a beamed nuclear source. A nuclear source with a strong flare or pulse about 6 10^3 yr before our present view is in principle possible, but does not account for the radio emission, velocity structure, or lack of stronger emission in other directions at this projected distance. Since virtually all plasmas seen in galaxies show filling factors much less than unity, the lower limit of 4 cm^{-3} is very conservative. Thus, photoionization by a flat nuclear continuum (one of strength sufficient to power the nuclear emission lines) is essentially ruled out.

A picture has been advanced for somewhat similar properties of M 51, by Ford et al. (1985), and in modified form by Goad and Gallagher (1985), in which optical and radio emission regions several hundred parsecs from the nucleus are powered by energy mechanically transmitted from the nuclear region in the form of jets or explosive events producing bubbles. We suggest a similar origin for at least this feature in NGC 2655: a jet, which might be seen at 6 cm, impinges on a cloud of low-density gas, producing both optical line emission and radio continuum in the boundary region.

We may examine the energy balance in this region from the Hα+[N II] and 6-cm size and emissivity measurements. The usual equipartition calculation leads to the following parameters for the radio-emitting plasma:

$$B = 6.5\ 10^{-5}\ \text{Gauss}$$
$$U_{\min} = 4\ 10^{-10}\ \text{erg cm}^{-3}$$
$$P = 2\ 10^{-10}\ \text{dyne cm}^{-2},$$

where the pressure includes both magnetic and charged-particle contributions. Similarly, for the thermal plasma responsible for optical line emission, a representative electron temperature of 10^4 K leads to

$$P = 3\ 10^{-11}\ \text{dyne cm}^{-2}$$

required by the [S II] $\lambda 6717/\lambda 6731$ ratio to be $< 1.4\ 10^{-10}$ at the limit of the measuring error, and

$$U_{\text{th}} = 6\ 10^{-11}\ \text{erg cm}^{-3}$$

similarly required to be less than 2.7 10^{-10} erg cm^{-3}. The absolute limits are so far from the "measured" values here because the density-sensitive [S II] line ratio approaches its low-density limit in this range, so that the measured errors lead to a large allowed range in N_e.

These values indicate that the pressures and energy content in the thermal and non-thermal plasmas are similar; the values for the non-thermal, radio-emitting material are higher, to an extent difficult to reconcile with measurement errors. Unless it is confined by, for example, magnetic structure, the radio plasma should be expanding or moving into the emission-line material. Here again, the ionization might be associated with shock fronts or with a locally generated ionizing continuum too weak for direct detection.

Somewhat similar features on a larger scale have been reported in several powerful radio galaxies (e.g., Tadhunter et al., 1987). In the case of PKS 2152–69, a continuum source probably sufficient to power the emission region is observed, while others such as PKS 0521–36 (Danziger et al., 1985) or the northern lobe of Coma A (van Breugel et al., 1983) show no such continuum source More sensitive searches for any such continuum, using higher spatial resolution or UV wavelengths, would be important in clarifying the details of the presumed interaction between these plasmas.

There is some evidence that transport of energy in a jet is involved in the ESE knot. The radio structure near the nucleus (Hummel et al., 1984; see also Fig. 4) shows bending jets, a plausible continuation of which connects on one side with the knot. By analogy with giant "classical" radio galaxies, a jet feeding the knot (in place of a more distant lobe) is not unexpected. The lower-resolution maps in Fig. 5 show some weak evidence for a connection, but we are unable to claim a fully convincing detection of a jet here. The energy is presumably transported to the knot somehow, suggesting the presence of a (relatively efficient) jet.

There is a significant offset between 6 cm and Hα peaks of the ESE knot. Using offsets from the optical nucleus, the northern component of the Hα emission is centered at (1950) $8^h49^m13^s.20 \pm 0.15$, $+78°24'41''.8 \pm 0''.4$ and the southern at $8^h49^m13^s.67$, $+78°24'40''.1$. The emission regions seen optically then fall on the outermost contours of the emission knot in Fig. 4, directly away from the nucleus. This is consistent either with bulk motion of the radio plasma compressing and exciting the optical emission-line gas, or with the proximity of the radio plasma in itself exciting the emission lines. The velocity structure seen in emission lines does suggest that this gas is being disturbed or disrupted by the radio plasma, on a timescale $\sim 10^6$ yr (from velocity spread and projected extent). Unless the 10^4 K gas is replenished (perhaps by sweeping up the interstellar medium), this is a transient, and rarely observable, stage in the evolution of the radio source.

5. Discussion

The optical properties of the nuclear region in NGC 2655 are unique among nearby galaxies, as regards both the structure and extent of gas related to the nucleus. The off-nucleus emission knot has close analogues only among more luminous and active systems. What, then, is special about NGC 2655? The optical and H I morphologies suggest that this galaxy has been dynamically disturbed. Patches of dust cross the optical image, roughly,along the projected minor axis, and the outermost regions in Palomar Sky Survey plates resemble ripples or shells such as may be formed in mergers of hot and cold stellar systems (see Quinn, 1984). The chaotic velocity structure in the surrounding H I (Shane, in preparation) also suggests the aftermath of a strong interaction. Since luminous radio galaxies frequently, show similar traces of mergers or interactions (Heckman et al., 1986), it is tempting to relate the unusual nuclear activity in NGC 2655 to the evidence for interaction or merger preserved in its outer regions.

While this hypothesis does not make detailed predictions, there are some features that are accounted for in a natural way. The presence of substantial gas over a wide region, and a relatively strong radio core, would both result from gas transferred from a former companion. The orientation of the loop seen in Hα might result from the orbital angular momentum of this companion, as preserved in the polar dust patches. It should be clear from this discussion that we have found unusual manifestations of activity in the nucleus of NGC 2655, perhaps related to recent accretion of a gas-rich companion galaxy. Our observations are not sufficient to determine the nature of all the features we have seen, but should indicate the important points and guide further work on this object.

References

Andrillat, Y., Souffrin, S., Alloin, D.: 1972, *Astron. Astrophys.* **19**, 405

van Breugel, W.J.M., Heckman, T., Butcher, H.R., Miley, G.: 1984, *Astrophys. J.* **277**, 82
van Breugel, W.J.M., Miley, G.K., Heckman, T.M., Butcher, H.R., Bridle, A.H.: 1985, *Astrophys. J.* **290**, 496
Clark, B.G.: 1980, *Astron. Astrophys.* **89**, 377
Crane, P.C.: 1977, Ph.D. diss., Massachussetts Institute of Technology
Dahari, O., Ford, H.C., Ciardullo, P., Jacoby, G., Crane, P.C.: 1986, *Bull. Am. Astron. Soc.* **18**, 640
Danziger, I.J., Shaver, P.A., Moorwood, A.F.M., Fosbury, R.A.E., Goss, W.M., Ekers, R.D.: 1985, ESO Messenger #39, 20
Filippenko, A.V., Halpern, J.G.: 1984, *Astrophys. J.* **285**
Filippenko, A.V., Sargent, W.L.W.: 1985, *Astrophys. J. Suppl.* **57**, 503
Ford, H.C., Butcher, H.R.: 1979, *Astrophys. J. Suppl.* **41**, 147
Ford, H.C., Crane, P.C., Jacoby, G.H., Lawrie, D.G., van der Hulst, J.M.: 1985, *Astrophys. J.* **293**, 132
Goad, J.W., Gallagher, J.S., III.: 1985, *Astrophys. J.* **247**
Heckman, T.M.: 1980, *Astron. Astrophys.* **81**, 152
Heckman, T.M., Smith, E.P., Baum, S.A., van Breugel, W.J.M., Miley, G.K., Illingworth, G.D., Bothun, G.D., Balick, B.: 1986, *Astrophys. J.* **311**, 526
Hummel, E., van der Hulst, J.M., Dickey, J.M.: 1984, *Astron. Astrophys.* **134**, 207
van der Hulst, J.M., Crane, P.C., Keel, W.C.: 1981, *Astron. J.* **86**, 1175
Joint IRAS Science Working Group 1985: Cataloged Galaxies and Quasars Observed in the IRAS Survey (Washington, D.C.: U.S. Government Printing Office)
Keel, W.C.: 1983, *Astrophys. J.* **269**, 466
Keel, W.C.: 1985a, *Nature* **318**, 43
Keel, W.C.: 1985b, in *Astrophysics of Active Galaxies and Quasi Stellar Objects*, ed. J.S. Miller (University Science Books, Mill Valley, California), p. 1
Quinn, P.J.: 1984, *Astrophys. J.* **279**, 596
Sandage, A.R., Tammann, G.: 1981, *A Revised Shapley Ames Catalog of Bright Galaxies* (Carnegie Institute, Washington)
Shane, W.W., Krumm, N.: 1983, in *Internal Kinematics and Dynamics of Galaxies*, *IAU Symp.* **100**, ed. E. Athanassoula, Reidel, Dordrecht, p. 105
Tadhunter, C.N., Fosbury, R.A.E., Binnette, L., Danziger, I.J., Robinson, A.: 1987, *Nature* **325**, 504
Thompson, A.R., Clark, B.G., Wade, C.M., Napier, L.J.: 1980, *Astrophys. J. Suppl.* **44**, 151
de Vaucouleurs, G., de Vaucouleurs, A., Corwin, H.G.: 1976, *Second Reference Catalog of Bright Galaxies*, University of Texas, Austin)